

THE HADRON SPECTRUM IN LATTICE QCD

G. Schierholz

Deutsches Elektronen-Synchrotron DESY, Hamburg

Abstract: I give a brief introduction to lattice QCD and discuss some of the recent calculations of the hadron mass spectrum. I also address the question of spontaneous chiral symmetry breaking which most obviously influences the character of the hadron spectrum.

I. Introduction

Recent months have seen considerable progress in understanding the hadron mass spectrum. This has required two developments: Firstly the construction of a theoretically appealing and phenomenologically reasonable fundamental field theory, QCD, and secondly the development of nonperturbative methods, the lattice Monte Carlo techniques, to solve and hence to give a real meaning to the QCD Lagrangian.

In this talk I shall introduce you to "lattice QCD" and discuss some of the recent calculations of the hadron mass spectrum.

The plan of the talk is as follows: After the introduction in this section I shall, in section 2, first discuss that part of the hadron spectrum that is composed primarily of the gluon degrees of freedom. These hadrons, the glueball states, are very much a prediction of QCD, and the absence of specific experimental information on these states provides us with the opportunity of making quantitative predictions that have no experimental bias. The dynamics that most obviously influences the character of the quark states is that of chiral symmetry and its spontaneous breaking. If QCD is to be a successful candidate theory it must reproduce this phenomenon. If it does not then the meson and baryon spectrum predicted by QCD will possess parity doubling and no very light pions, in damaging contrast to the experimental situation. In section 3 I shall convince you that QCD indeed breaks its (zero quark mass) chiral symmetry dynamically. This is largely a question of the lattice size. In section 4 finally I will present very recent results of a Monte Carlo calculation of the meson and baryon mass spectrum on a $10^3 \times 16$ lattice which we have checked to be large enough to accommodate the dynamics of spontaneous chiral symmetry breaking and the hadrons themselves. I shall conclude with some remarks in section 5.

Lattice gauge theory⁽¹⁾

For the sake of simplification let us for the moment regard only the pure gauge theory. The starting point is the Feynman path in-

integral representation⁽²⁾ in Euclidean space-time

$$Z = \int [dA_\mu(x)] e^{-\frac{1}{2g^2} \int d^4x \text{Tr}(F_{\mu\nu} F_{\mu\nu})} , \quad (1)$$

where the field strength tensor is

$$F_{\mu\nu} = \partial_\mu A_\nu - \partial_\nu A_\mu + [A_\mu, A_\nu]. \quad (2)$$

Note that the coupling has been absorbed into the matrix-valued vector field $A_\mu(x)$:

$$A_\mu(x) = g A_\mu^a(x) T^a, \quad (3)$$

where the $A_\mu^a(x)$ are the gauge potentials and the T^a are a representation of the $SU(3)$ Lie algebra.

As it stands the representation (1) is incomplete. Any attempt at a calculation will encounter ultraviolet infinities. The conventional way to deal with this problem is to add to (1) a regularization prescription. That is, the theory is first mutilated by the arbitrary removal of the offending high momentum / short distance components of the fields, and then these components are systematically reintroduced while varying the coupling in such a way as to keep the theory finite. That means that beyond a certain momentum the reintroduction of the even higher momentum components will not affect the low energy physics. To implement the regularization procedure one must specify a momentum p_0 (distance a) such that momentum components higher than p_0 (distances smaller than a) are to be thrown away, and then the bare coupling g^2 in (1) is effectively the coupling on the size scale p_0^{-1} (a). We then take $p_0 \rightarrow \infty$ ($a \rightarrow 0$) varying $g^2(p_0)$ ($g^2(a)$) so as to keep the low-energy (large distance) physics unchanged. This necessarily breaks the scale invariance of the theory.

The standard regularization procedure in perturbative calculations is dimensional regularization⁽³⁾. This is however of no use for the calculation of nonperturbative quantities such as the hadron masses. An alternative procedure to remove high momenta/small distances is by discretising space-time. If we put the theory onto a lattice of spacing a we automatically restrict all the components of the momentum to be less than or equal to

$$p_0 = \frac{\pi}{a} \quad . \quad (4)$$

To recover the full theory we let $a \rightarrow 0$. Once a is much less than the dynamical lengths in the theory, characterized by some correlation length ξ , the physics of the theory should remain unchanged as $a \rightarrow 0$ as long as we vary g^2 with a according to the usual (two-loop) renormalization group formula

$$g^2(a) = \frac{16\pi^2}{11\ln(a\Lambda)^{-2} + \frac{102}{11} \ln\ln(a\Lambda)^{-2}} \quad , \quad (5)$$

which (to two loops) is the same for all regularization procedures apart from the Λ parameter which can be related to the more familiar Λ_{mom} via a perturbative calculation. For calculational convenience we also wish to confine space-time to a finite volume, say L lattice spacings in each direction. Then if $\xi \ll La$ the physics should be the same as for the infinite volume limit. The purpose of this discussion is to make the point that lattice QCD is not some kind of approximation to "true" QCD but, when treated in the appropriate region of parameters

$$a \ll \xi \ll La \quad , \quad (6)$$

precisely is "true" QCD.

The basic geometric facets of the lattice are the sites, the links, the plaquettes, etc. A vector gauge field belongs most naturally to the links joining neighbouring sites

$$A_\mu(x) \rightarrow U_\mu(n) = e^{iaA_\mu} \approx 1 + iaA_\mu \quad . \quad (7)$$

For small a the U_μ are just the elementary line integrals of the continuum gauge potential. A tensor field could naturally be associated with a plaquette. With fermions the situation is less straightforward, and this contributes to the difficulties in calculating with them.

The partition function (1) then becomes

$$Z = \int \prod_{n,\mu} [dU_\mu(n)] e^{-S(U)} \quad , \quad (8)$$

where the measure is the Haar invariant measure over the gauge group SU(3). The action $S(U)$ must reproduce the usual continuum Euclidean action (1-3) in the limit $a \rightarrow 0$. An example is the Wilson action

$$S(U) = \beta \sum_n \left(1 - \frac{1}{3} \text{Tr} \square\right), \quad \beta = \frac{6}{g^2}, \quad (9)$$

where $\text{Tr} \square$ means taking the trace of the matrix obtained by multiplying together the four matrices U_μ on the links forming the plaquette.

Monte Carlo solution

Formulated in Euclidean space-time the lattice regulated gauge theory looks like a statistical mechanical system with a Boltzmann factor e^{-S} which suggests⁽⁴⁾ using methods developed for solving such systems. The method that interests us here is the Monte Carlo technique⁽⁵⁾.

Suppose we want to calculate the vacuum expectation value

$$\langle O(U) \rangle = \frac{1}{Z} \int_{n, \mu} [dU_\mu(n)] O(U) e^{-S(U)} \quad (10)$$

The essence of the Monte Carlo method then is to generate a sequence of (typical) gauge field configurations according to the distribution $n, \mu [dU_\mu(n)] e^{-S(U)}$. Suppose we have N such configurations

$$\{U_\mu(n)\}_{i=1, \dots, N} \quad (11)$$

Then the vacuum expectation value (10) is given by

$$\langle O(U) \rangle \approx \frac{1}{N} \sum_{i=1}^N O(\{U_\mu(n)\}_i) \quad (12)$$

which becomes exact as $N \rightarrow \infty$.

2. Glueball Mass Spectrum (6)

We turn now to the calculation of the masses of the glueball states. All (SU(3)) calculations so far have been done in the quenched approximation, that is without fermion loops, using the Wilson action(9).

We first form wave-functionals with the desired J^{PC} quantum numbers. Since the theory is confining the glueballs are colour singlets, and an (over)complete set of colour singlet operators is given by the set of all closed loops. To make the operators have the required J^{PC} properties we take suitable linear combinations of rotations and reflections and real or imaginary parts (the real part having $C = +1$, the imaginary part having $C = -1$). In Fig. 1 I show for example the 2×2 loop and the linear combinations of this loop that project onto $J^{PC} = 0^{++}$ and $J^{PC} = 2^{++}$.

Computational procedure

The by now standard technique⁽⁷⁾ for calculating glueball masses proceeds roughly as follows⁽⁸⁾. Take the trial glueball wave-functional, $\Phi(\vec{n}, t)$, constructed as above with the desired J^{PC} properties and centred on the site (\vec{n}, t) . Make the $\vec{p}=0$ translation invariant sum

$$\Phi(\vec{p}=0, t) = \sum_{\vec{n}} \Phi(\vec{n}, t) \quad (13)$$

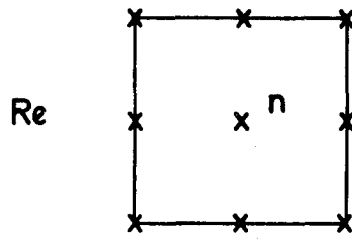
and measure the correlation function

$$\begin{aligned} \Gamma_t &= \langle \Phi(\vec{p}=0, t) \Phi(\vec{p}=0, 0) \rangle \\ &= \langle \Phi(\vec{p}=0, 0) e^{-Ht} \Phi(\vec{p}=0, 0) \rangle \\ &= \sum_{n=0}^{\infty} e^{-mn t} |\langle \Omega | \Phi | n \rangle|^2, \end{aligned} \quad (14)$$

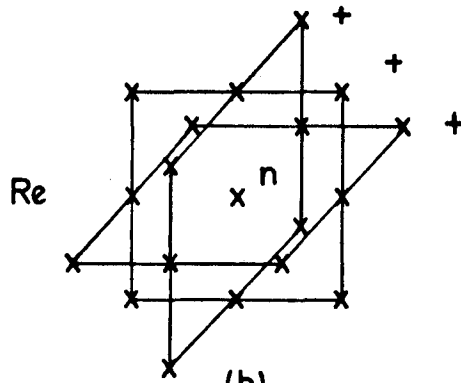
where $|\Omega\rangle$ is the vacuum. Vary Φ over a class of wave-functionals to obtain a large enough projection onto the desired glueball state so that Γ_t is dominated by the lowest mass glueball propagator for $t \geq a$. Then obtain the lowest glueball mass from

$$ma = \ln \left\{ \frac{\Gamma_{(n-1)a}}{\Gamma_{na}} \right\}. \quad (15)$$

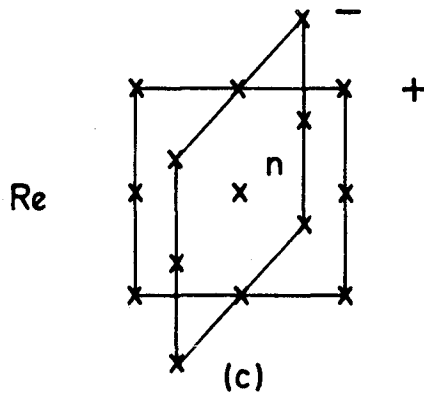
The choice of n will depend on the purity of the wave-functional (as to the admixture of higher excited states). Generally $n = 2$ or $n = 3$



(a)



(b)



(c)

Fig.1: (a) A 2×2 loop of link matrices, (b) a 0^{++} combination of 2×2 loops, (c) a 2^{++} combination of 2×2 loops.

will be large enough at present values of β to make m_1, m_2, \dots die away in equ. (14).

When are we in the continuum limit?

As I have indicated in the introduction we will have to do our calculations at sufficiently small lattice spacings such that the masses we obtain are indeed those of the continuum theory. In practice one assumes that the lattice spacing is small enough to be given by the perturbative formula

$$a(\beta) = \frac{83.5}{\Lambda_{\text{mom}}} \exp\left(-\frac{4\pi^2}{33} \beta\right) \left(\frac{8\pi^2}{33} \beta\right)^{\frac{51}{12\pi}}, \quad (16)$$

i.e. the inverse of (5), where the factor 83.5 comes from having replaced the lattice Λ parameter by the more conventional Λ_{mom} ⁽⁹⁾. A criterion for being in the continuum region then is that if we redo the calculation at larger values of β (smaller lattice spacings a), the dimensionless quantity ma (equ.(15)) we calculate should scale like $a(\beta)$. In other words m should be the same in units of Λ_{mom} . The problem with this criterion is that there are possibly higher order corrections to (16) which might become visible as the errors of the Monte Carlo calculations decrease with time. An alternative criterion which avoids (16) is that the ratio of masses or the ratio of mass to (string tension)² is independent of β .

The lattice spacing in physical units

The final step in calculating the glueball masses is to express these masses in MeV units to make contact to the real world (i.e. we must know a in MeV^{-1}). In principle we could use (16) with Λ_{mom} from deep inelastic experiments. However such values of Λ_{mom} are notoriously ill determined. The absence of any firm experimental glueball candidates (though recently two glueball candidates have been announced⁽¹⁰⁾) rules out to normalize any one of the calculated glueball masses to experiment. Instead one can calculate (say) the ρ mass and use its experimental value to set the scale of $a(\beta)$, provided that the calculated hadron spectrum comes out reasonably well. Such a calculation

exists⁽¹¹⁾ (see below) and we shall use it. One could also normalize to calculations of the string tension⁽¹²⁾, the gluon condensate⁽¹³⁾ $\langle \frac{\alpha_s}{\pi} F_{\mu\nu} F_{\mu\nu} \rangle$ or the chiral condensate⁽¹⁴⁾ $\langle \bar{\psi}\psi \rangle$. Since our mass calculations will be predominantly from $\beta \sim 5.7$ we shall center our analysis around this value (which should be borne in mind as the two-loop perturbative formula (16) is not likely to be exactly valid). Using (16) we obtain

from	$\Lambda_{\text{mom}}(\beta \sim 5.7)$ MeV
rho mass ⁽¹¹⁾ , m_ρ	210 ± 30
string tension ⁽¹²⁾ , $\sqrt{K} = 400$ MeV	230 ± 30
gluon condensate ⁽¹³⁾ , $\langle \frac{\alpha_s}{\pi} F_{\mu\nu} F_{\mu\nu} \rangle = (336 \pm 10 \text{ MeV})^4$ ⁽¹⁵⁾	180 ± 20
chiral condensate ⁽¹⁴⁾ , $\langle \bar{\psi}\psi \rangle_{\text{inv}} = (225 \pm 25 \text{ MeV})^3$ ⁽¹⁶⁾	195 ± 25

This gives us consistently

$$\Lambda_{\text{mom}} \approx 200 \text{ MeV} \quad (17)$$

and

$$a(\beta=5.7) = 1.37 \text{ GeV}^{-1} = 0.28 \text{ fermi.} \quad (18)$$

Results

On a hypercubic $L_s^3 \times L_t$ lattice (of $L_s(L_t)$ lattice spacings in the spacial (time) direction) the inequality (6) reads in a more graphic language

$$a \ll D \ll \frac{1}{2} \min(L_s a, L_t a) \quad (19)$$

where (here) D is the glueball diameter. The factor $\frac{1}{2}$ comes from using the periodic boundary conditions to reduce the obvious finite volume effects. In order for the calculation of hadron properties to be credible we also require the temperature ($= 1/L_t a$) to be much smaller than the deconfinement temperature of $\approx 200 \text{ MeV}$ ⁽¹⁷⁾. To realize (19) we need at least a rough estimate of the glueball size.

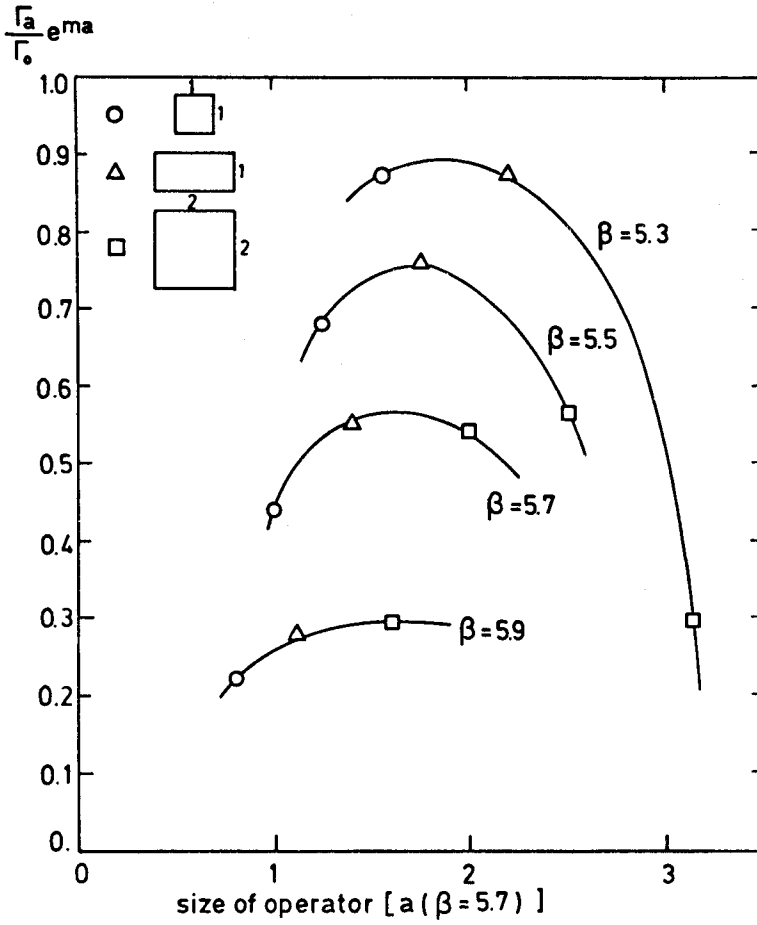


Fig.2: Γ_a/Γ_0 for various operators versus the size of the operators in units of the $\beta = 5.7$ lattice spacing.

This may be found in ref.18 where we have calculated Γ_a/Γ_0 for several basic loops of differing sizes. It should have a maximum at approximately the glueball diameter. The result of the calculation done at several values of β I have shown in Fig. 2, where the geometrical loop sizes have been expressed in terms of the lattice spacing $a(\beta=5.7)$ using (16). We find

$$D \approx (1.5-2.0) a(\beta=5.7) \approx 0.5 \text{ fermi.} \quad (20)$$

From (20) we conclude that (19) is more or less satisfied for $5.3 \leq \beta \leq 5.9$ (albeit with an optimistic interpretation of the strong inequalities in (19)) for $L_s, L_t = 4$ and accordingly for larger lattices. If we now pick $L_t = 8$ then the temperature varies from ≈ 60 to ≈ 120 MeV in this range of β values which is also well below the deconfinement temperature.

The calculation of glueball masses requires high (Monte Carlo) statistics. For this reason almost all of the work has been on lattices as small as possible, typically $L_s^3 \times L_t = 4^3 \times 8$. To be sure that finite size effects are small it is important to also have a glueball calculation on a much larger lattice. Such a calculation now exists⁽¹⁹⁾, showing that the results on an 8^4 lattice do not differ very much from those on $4^3 \times 8$ lattices as we shall see.

We have systematically calculated^(18,20) the masses of the supposedly low-lying glueball states. We find four light glueballs, the 0^{++} , 2^{++} , 0^{-+} and the oddball 1^{-+} . In addition to our work there have also been estimates for the bulk of the glueball spectrum by Berg and Billoire^(21,22) and a 0^{++} estimate by Michael and Teasdale⁽²³⁾.

0^{++} :

In Fig.3 I have plotted the statistically best $L_s=4$ results⁽¹⁸⁾ together with some results on a $5^3 \times 8$ lattice⁽²²⁾ and those on an 8^4 lattice⁽¹⁹⁾. All the estimates come from Γ_{2a}/Γ_a except for $\beta=5.9$ where Γ_{3a}/Γ_a has been used. We observe that any systematic variation of $m(0^{++})$ between $\beta=5.3$ and $\beta=5.9$ is less than 20%. In this same range of β the lattice spacing (16) decreases by a factor of ≈ 2 , which leads us to conclude that we are seeing evidence for the calculated 0^{++} mass being that of the continuum theory.

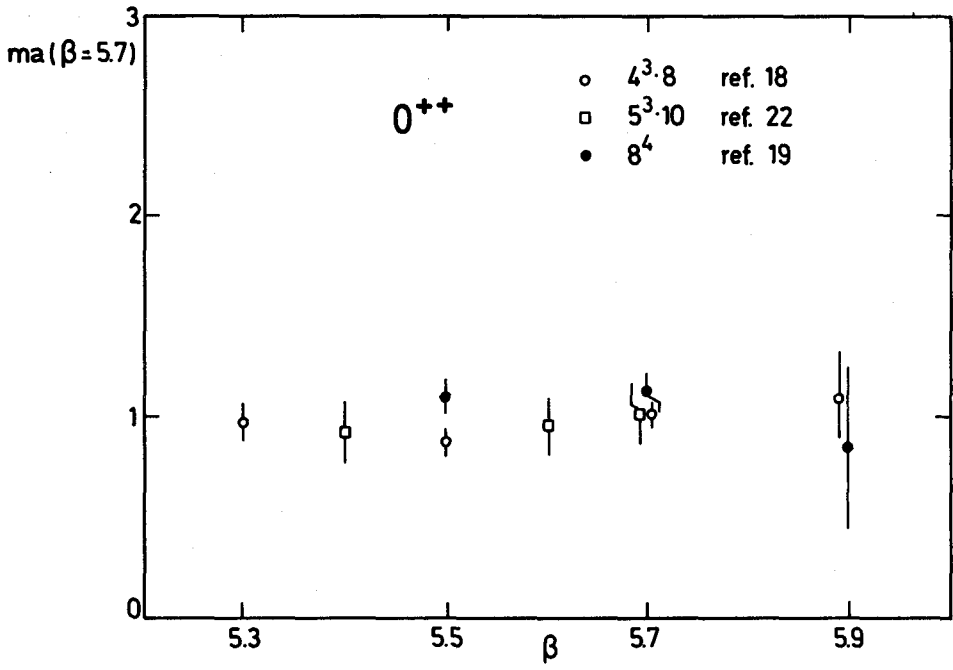


Fig.3: 0^{++} mass on $4^3 \times 8$, $5^3 \times 8$ and 8^4 lattices in units of a^{-1} ($\beta=5.7$).

If we compare $m(0^{++})$ obtained on $4^3 \times 8$ and 8^4 lattices we find that any changes are small. The largest change is at $\beta = 5.5$ which might be associated with the diminishing of the specific heat peak⁽²⁴⁾ with increasing lattice size⁽¹³⁾.

2^{++} :

In Fig.4 I have plotted our results obtained on $4^3 \times 8$ ⁽¹⁹⁾ and 8^4 ⁽¹⁸⁾ lattices. The systematic variation of $m(2^{++})$ between $\beta = 5.3$ and $\beta = 5.9$ is $\approx 30\%$ which again is much smaller than the $\approx 100\%$ decrease of the lattice spacing in this range of β . This gives us confidence that also the calculated 2^{++} mass is that of the continuum. The masses in Fig.4 show no finite size effects outside the errors.

The 2^{++} glueball mass has also been calculated by Berg and Billoire⁽²²⁾. They claim to see no continuum scaling behaviour. For a possible resolution of this discrepancy I refer the interested reader to refs. 6, 18.

0^{-+} and 1^{-+} :

There are claims⁽¹⁸⁾ for a light pseudoscalar 0^{-+} glueball and a light 1^{-+} oddball. Oddballs are glueballs which have quantum numbers not accessible to a quark-antiquark pair. So far there is no numerical test of continuum behaviour or of finite size effects for either state. The presumption is that finite size effects will be small and that the masses have reached their continuum limit which needs however to be checked.

Summary of masses:

The calculated masses of the low-lying glueball states are

$$\begin{aligned}
 m(0^{++}) &= 770 \pm 40 \text{ MeV,} \\
 m(0^{-+}) &= 1420 + \begin{matrix} 240 \\ - 170 \end{matrix} \text{ MeV,} \\
 m(2^{++}) &= 1670 + \begin{matrix} 110 \\ - 90 \end{matrix} \text{ MeV,} \\
 m(1^{-+}) &= 1730 \pm 220 \text{ MeV.}
 \end{aligned}
 \tag{21}$$

The scale used is $\Lambda_{\text{mom}} = 200 \text{ MeV}$ as I have discussed above. For the experimental status of the search for glueballs see ref. 25.

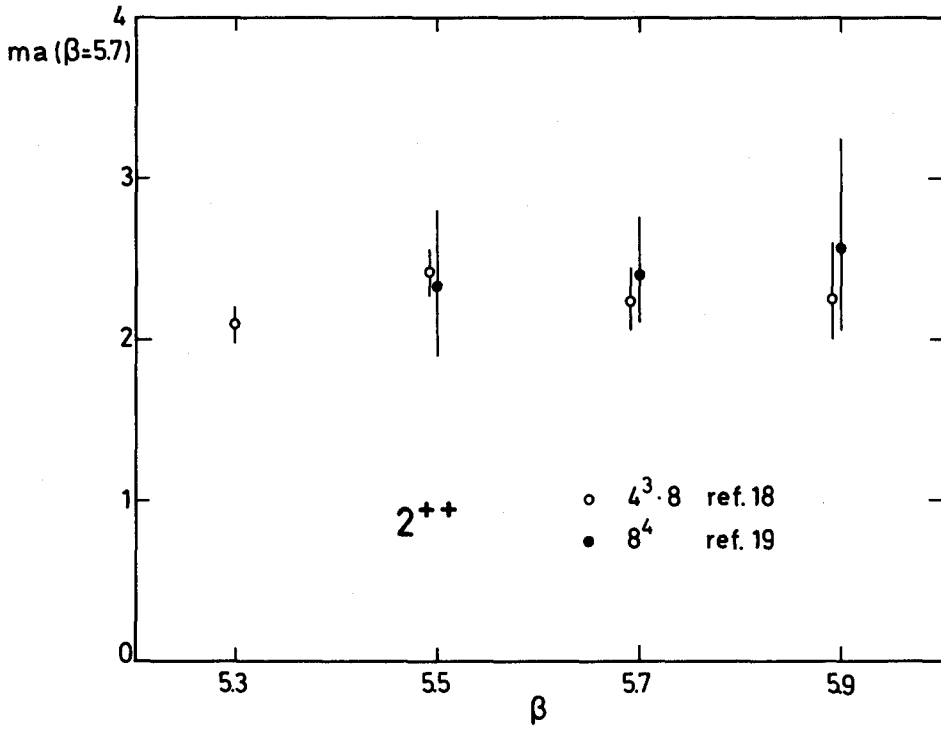


Fig. 4: 2^{++} mass on $4^3 \times 8$ and 8^4 lattices in units of $a^{-1}(\beta=5.7)$.

3. Evidence for Spontaneous Chiral Symmetry Breaking?

Until recently it was not established whether QCD breaks its chiral symmetry dynamically or not. This problem is made difficult by its nonperturbative nature and required to go new roads to resolve it: the lattice Monte Carlo method.

Fermions on the lattice

So far we have dealt with the pure gauge theory only. To put quarks onto the lattice is less straightforward, and I refer the reader for a more detailed discussion to the literature⁽²⁶⁾.

For the fermions we want an action which explicitly possesses a continuous chiral symmetry on top of reproducing the usual continuum Euclidean action in the limit $a \rightarrow 0$. The Wilson fermion action⁽²⁷⁾ breaks all chiral symmetries by irrelevant operators, and there is no evidence that it has recovered chiral symmetry (enough to break it spontaneously) in the range of couplings numerically accessible at present. The naive action

$$S(\bar{\Psi}, \Psi, U) \equiv -\bar{\Psi}[M(U)+2ma]\Psi \quad (22)$$

$$= - \sum_{n, \mu} \bar{\Psi}(n) \gamma_{\mu} [U_{\mu}(n) \Psi(n+\mu) - U_{\mu}^{\dagger}(n-\mu) \Psi(n-\mu)] - 2ma \sum_n \bar{\Psi}(n) \Psi(n)$$

has an obvious chiral symmetry when $m = 0$ but describes 16 "flavours" instead of one. Unfortunately a local, explicitly chiral invariant formulation of the fermion action on the lattice without species doubling does not exist⁽²⁸⁾. The next best choice are Kogut-Susskind staggered fermions⁽²⁹⁾ which are identical to naive fermions if one only excites one of their 4 decoupled modes and describe 4 flavours. This relationship is most clearly seen if we decompose the (anti-hermitean) matrix M into

$$M = \Gamma M \Gamma^{\dagger}, \quad (23)$$

where Γ is a unitary block diagonal matrix containing all the γ matrices⁽³⁰⁾, and write

$$\psi = \Gamma \chi \quad . \quad (24)$$

Then the action (22) becomes

$$S(\bar{\chi}, \chi, U) = -\bar{\chi} [M(U) + 2ma] \chi \quad , \quad (25)$$

where the 4 Dirac components of χ decouple. This allows us to work with a single component fermion field, thereby reducing the number of degrees of freedom by a factor of 4. The action (25) reduced to a single component χ field is the action for staggered fermions. The interpretation as 4-flavoured lattice fermionic fields⁽³¹⁾ follows by dividing the lattice into hypercubes and defining a new field (of 4 Dirac components x 4 flavours) to be $\chi(n)$ times an appropriate phase factor at each of the 16 corners of the hypercube. The matrix M is a $N \times N$ sparse complex matrix where $N = 3 L_s^3 \times L_t$. We shall use antiperiodic boundary conditions for the fermion fields.

The action for staggered fermions has a $U(4) \times U(4)$ symmetry for $m=0$ in the continuum limit. At finite lattice spacing the $U(4)$ chiral symmetry is explicitly broken down to $U(1)$. The important point is that there is an explicit continuous chiral $U(1)$ symmetry for which

$$\langle \bar{\psi} \psi(m) \rangle = \frac{3}{N} \langle \text{Tr}(M + 2ma)^{-1} \rangle \quad (26)$$

is an order parameter, and this $U(1)$ is not the anomaly afflicted piece of $U(4)$ but belongs to the $SU(4)$ ⁽³²⁾.

In what follows we shall have to restrict ourselves to the quenched approximation as in case of the glueball calculation. That means the vacuum expectation values (cf. eqs. (10) - (12)) of interest are defined by averaging over gauge field configurations which are in equilibrium with the pure gauge field action (9). So far nobody has mastered to include fermion loops in generating "snapshots" of the vacuum in an efficient way.

$$\langle \bar{\psi} \psi \rangle$$

The usual criterion for chiral symmetry breaking is that the chiral condensate (26) should not vanish as $m \rightarrow 0$. Since a finite lattice

(being a system with a finite number of degrees of freedom) will, given enough time, rotate through all the degenerate minima of the effective potential so that one obtains $\langle \bar{\psi}\psi(m \rightarrow 0) \rangle = 0$ even if the symmetry is dynamically broken, the correct criterion is that

$$\lim_{m \rightarrow 0} \lim_{\text{volume} \rightarrow \infty} \langle \bar{\psi}\psi(m) \rangle \neq 0. \quad (27)$$

To check whether (27) holds or not one must calculate (26) for several different lattice volumes. The condensate should tend to an envelope which has a nonzero intercept at $m = 0$. The largest volumes should be such that the mass at which $\langle \bar{\psi}\psi(m) \rangle$ breaks away from the envelope to collapse to zero is much smaller than the gauge theory scale, $O(\Lambda_{\text{mom}})$, to demonstrate that this is a kinematic rather than a dynamic effect. It is clear that such a calculation requires great accuracy at very small quark masses.

To show that the spontaneous breaking is a continuum property one must do the calculation over a range of β and demonstrate the correct continuum renormalization group behaviour for (27).

The numerical problem we are faced with in (26) is that of calculating the inverse or the eigenvalues of a very large complex matrix. The best method we know at present for obtaining (selected rows of) the inverse is the conjugate gradient method⁽³³⁾, and the best method we know for obtaining the eigenvalues is the Lanczos algorithm⁽³³⁾. In the present context there are good reasons for preferring the latter method.

Results⁽¹⁴⁾

In Fig.5 I have plotted the calculated $\langle \bar{\psi}\psi(m) \rangle$ for $4^3 \times 8$, $6^3 \times 8$ and 8^4 lattices at $\beta=5.7$. Also shown is $\langle \bar{\psi}\psi(m) \rangle$ at 3 mass values for a $10^3 \times 16$ lattice. These values come from a hadron spectrum calculation⁽¹¹⁾ using the conjugate gradient algorithm. We observe that a $4^3 \times 8$ lattice shows no significant signal of spontaneous chiral symmetry breaking. As we increase the lattice we see a clear envelope developing, and this envelope has a nonzero intercept at zero quark mass. Comparing our 8^4 and $10^3 \times 16$ results we see that for this

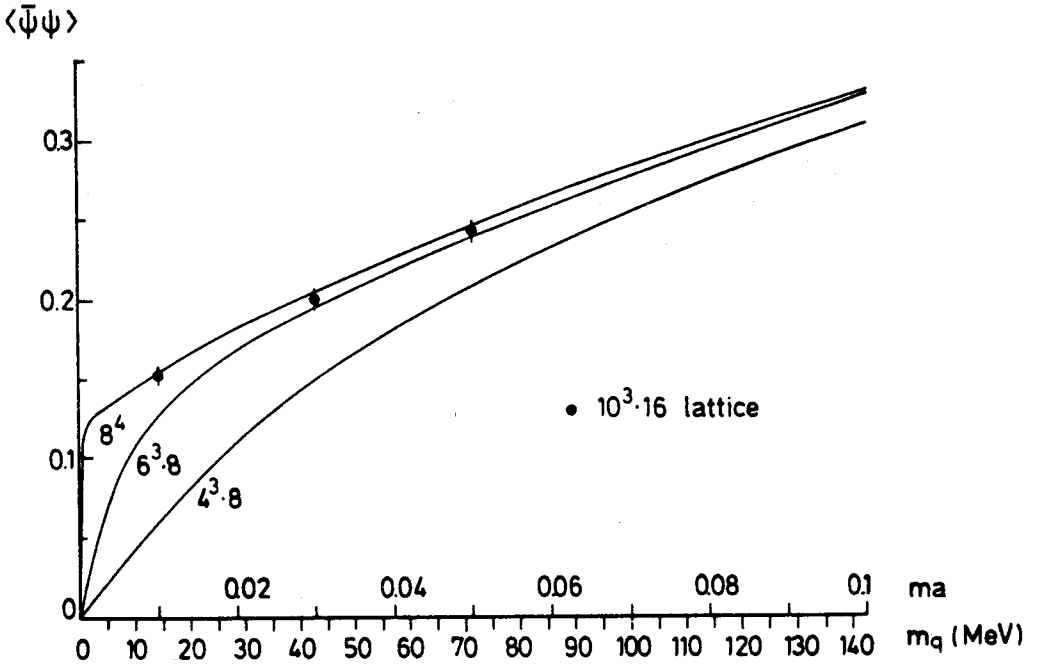


Fig.5: $\langle \bar{\Psi}\Psi \rangle$ as a function of the bare (renormalization group invariant) quark mass ma (m_q) obtained on the $4^3 \times 8$, $6^3 \times 8$ and 8^4 lattice at $\beta = 5.7$. The solid circles come from the hadron spectrum calculation on the $10^3 \times 16$ lattice to be described later on.

physics an 8^4 lattice at $\beta \sim 5.7$ is effectively of infinite volume down to $ma \approx 0.01$. The break-away occurs at a quark mass $ma = 0(0.002)$ where it is obviously a kinematic effect. The bare quark mass m is related to the more physical renormalization group invariant quark mass⁽¹⁶⁾ m_q also indicated in Fig.5 by

$$m_q = \alpha_{\text{mom}}^{-\frac{4}{11}} m, \quad \alpha_{\text{mom}} = \frac{g^2 \text{mom}}{4\pi}. \quad (28)$$

To demonstrate that this is a continuum effect we have calculated $\langle \bar{\psi}\psi(m) \rangle$ for values of β from 0 to 5.9. We find that we have roughly a linear dependence on ma for $ma \lesssim 0.1$ until the break-away to zero occurs. We obtain $\langle \bar{\psi}\psi(0) \rangle$ by extrapolating this linear dependence to $ma=0$. Our values for $\langle \bar{\psi}\psi(0) \rangle$ are plotted in Fig.6. We can see the strong coupling behaviour⁽³⁴⁾ at low β , a transition region between $\beta = 4$ and 5.1 and very clear continuum (asymptotic freedom) behaviour for $\beta > 5.1$.

Our calculated (dimensionless) $\langle \bar{\psi}\psi \rangle$ can be expressed in terms of the continuum (dimensionful) renormalization group invariant $\langle \bar{\psi}\psi \rangle_{\text{inv}}$ by

$$\langle \bar{\psi}\psi \rangle = 2\alpha_{\text{mom}}^{-\frac{4}{11}} a^3 \langle \bar{\psi}\psi \rangle_{\text{inv}} \quad (29)$$

(the normalization uses 4 flavours). Using (16) and $\Lambda_{\text{mom}} = 200$ MeV (see (17) and above) I have plotted $\langle \bar{\psi}\psi \rangle_{\text{inv}}^{1/3}$ as a function of β in Fig.7. We see that we have good numerical agreement with the experimental value⁽¹⁶⁾ for $\langle \bar{u}u \rangle$.

4. Meson and Baryon Masses

We may hope now that the Kogut-Susskind fermionic lattice QCD action (25) will also provide a realistic description of the meson and baryon spectrum.

The fact that the promise of the early calculations⁽³⁵⁾ on very small lattices was not fulfilled by later, more detailed work⁽³⁶⁾ emphasized for us the dangers of using Wilson fermions. This was widely interpreted at the time as a problem of finite size effects⁽³⁷⁾, with the cure to be found by increasing the lattice size. That finite size

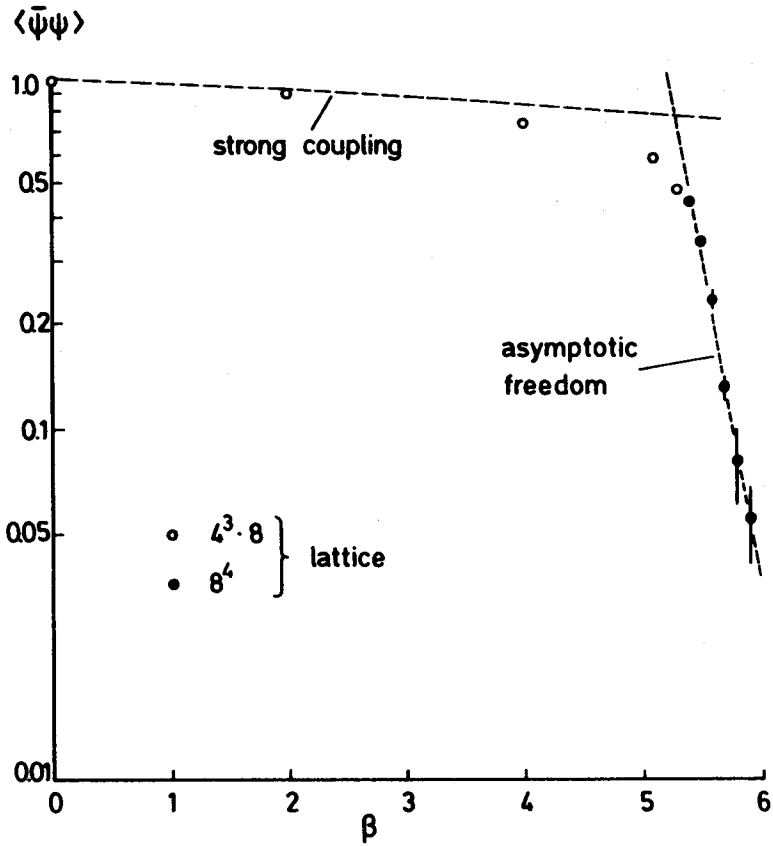


Fig. 6: The intercept $\langle \bar{\psi}\psi \rangle$ for various values of β together with the $O(1/d)$ strong coupling and scaling (asymptotic freedom) curves.

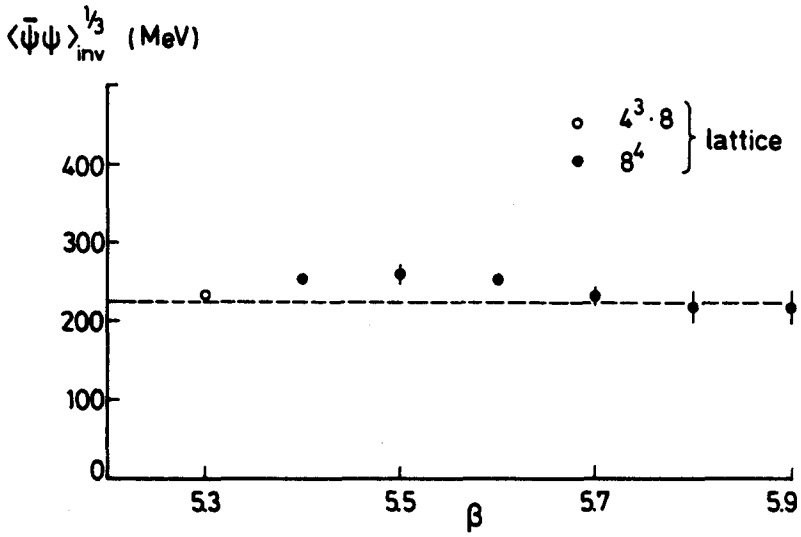


Fig.7: The renormalization group invariant $\langle \bar{\psi}\psi \rangle_{\text{inv}}^{1/3}$ for $5.3 = \beta = 5.9$.
The dashed line represents the experimental value $\langle \bar{u}u \rangle = 225$ (± 25) MeV.

effects were part of the problem was clear. There is however also the possibility that these effects are being magnified by the forced extrapolation of mass calculations performed at large pion masses to zero pion mass in a theory that has not yet developed a chiral symmetry that can be spontaneously broken. Recent calculations with Wilson fermions on large $10^3 \times 20$ ⁽³⁸⁾ and 16^4 ⁽³⁹⁾ lattices have in fact shown that the problems are still there.

In continuation of our work on chiral symmetry breaking we have calculated the meson and baryon masses on a $10^3 \times 16$ lattice ⁽¹¹⁾. We have performed our calculation at $\beta=5.7$. There the spatial extent of our lattice is (cf. equ. (18)

$$10a(\beta=5.7) = 2.8 \text{ fermi} \gtrsim 2D, \quad (30)$$

where D is a typical meson or baryon diameter. This seems a reasonably large space for the hadron on a lattice (with antiperiodic fermionic boundary conditions).

I shall not go into details of the flavour structure of staggered fermions. All what we need for calculating meson and baryon masses are operators that project onto meson and baryon states made out of the desired combination of flavours. The local operators

$$\bar{\Psi}(n)\gamma_5\Psi(n), \bar{\Psi}(n)\gamma_\mu\Psi(n), \bar{\Psi}(n)\gamma_5\gamma_\mu\Psi(n), \bar{\Psi}(n)\Psi(n), \bar{\Psi}(n)\sigma_{\mu\nu}\Psi(n) \quad (31)$$

and

$$\epsilon_{ABC}(\psi^A(n)\gamma_5\psi^B(n))\psi^C(n), \epsilon_{ABC}(\psi^A(n)\gamma_\mu\psi^B(n))\psi^C(n) \quad (32)$$

will do this job with $\psi(n) = \Gamma(n)\chi(n)$, $\chi(n)$ being a single component fermion field (cf. equ.(25)). The operators (31) project onto the ⁽³²⁾ π, ρ, A_1, ϵ (i.e. the $(I,J)^{PC} = (0,0)^{++}$ singlet) and B , respectively, while (32) project onto the nucleon (N) and Δ and their negative parity partners. This then leads us to evaluate the propagators ($\Gamma(0) = 1$)

$$\begin{aligned}
M_{PS}(t) &= \sum_{\vec{n}} \frac{1}{4} \text{Tr}(\gamma^+ (n) \gamma_5 \Gamma(n) \gamma_5) \langle \bar{\chi}(n) \chi(n) \bar{\chi}(0) \chi(0) \rangle \\
&\quad t=n_4 a \\
&= \sum_{\vec{n}} \langle |G^{AB}(n)|^2 \rangle = c_\pi (e^{-m_\pi t} + e^{-m_\pi(16a-t)} + \dots), \\
&\quad A, B \\
&\text{etc.}
\end{aligned} \tag{33}$$

where

$$G^{AB}(n'-n) = [(M+2ma)^{-1}]_{nn'}^{AB} \tag{34}$$

We have used the conjugate gradient algorithm⁽³³⁾ to calculate the quark propagators (34). As before we work in the quenched approximation. That is the meson and baryon propagators (33) are sampled over a set of gauge field configurations in equilibrium with the action (9).

The result we obtain for the pion mass is shown in Fig.8. We find that $m_\pi^2 \sim m_q$, which is what one expects for a Goldstone pion. The dashed line in Fig.8 is parameterized by

$$(m_\pi a) = 7.60 ma. \tag{35}$$

Using $\Lambda_{\text{mom}} = 200 \text{ MeV}$ again we infer from (35) that the pion takes its experimental mass value for $ma \approx 0.005$, which corresponds to a renormalization group invariant quark mass of

$$m_q \approx 7 \text{ MeV} \tag{36}$$

This is the mass value one also obtains from current algebra⁽¹⁶⁾. The results for m_ρ , m_{A_1} , m_ϵ and the nucleon mass m_N are shown in Fig.9. The calculated hadron masses can be interpolated by the linear mass fits

$$\begin{aligned}
m_\rho a &= 0.98 + 4.10 ma, \\
m_{A_1} a &= 1.61 + 3.30 ma, \\
m_\epsilon a &= 0.88 + 5.70 ma, \\
m_N a &= 1.21 + 9.00 ma,
\end{aligned} \tag{37}$$

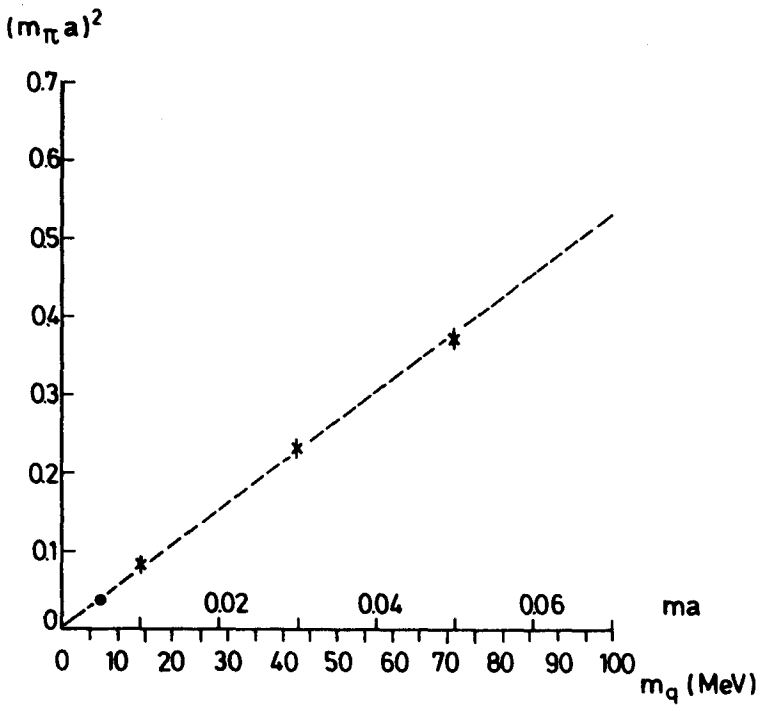


Fig.8: $(m_\pi)^2$ as a function of ma (m_q). The solid circle on the linear extrapolation curve marks the position of the physical pion, from which we can read off the value of the quark mass m_q .

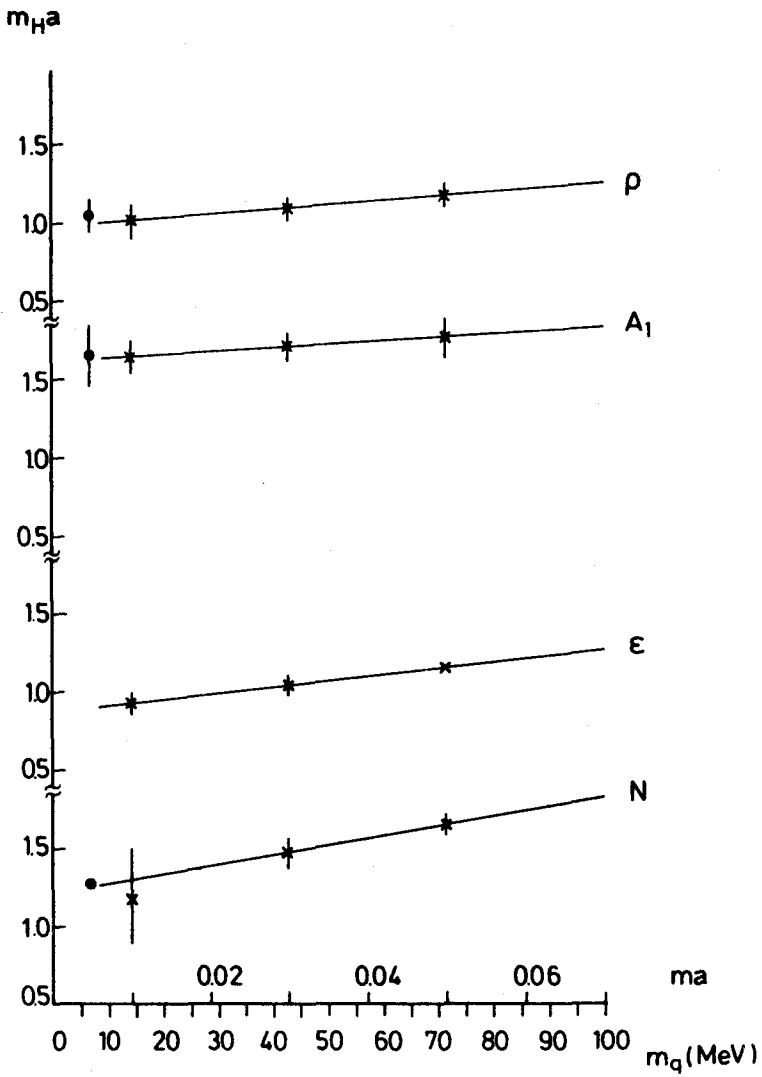


Fig.9: The hadron masses, m_{Ha} , as a function of m_q (m_q). The solid circles at the physical quark mass indicate their experimental values.

which correspond to the solid lines in Fig.9. We shall use (37) now to evaluate m_ρ , m_{A_1} , m_ϵ and m_N at the physical quark mass (36). For our usual $\Lambda_{\text{mom}} = 200$ MeV and taking the statistical errors properly into account we obtain

$$\begin{aligned} m_\rho &= (730 \pm 90) \text{ MeV}, \\ m_{A_1} &= (1119 \pm 90) \text{ MeV}, \\ m_\epsilon &= (660 \pm 50) \text{ MeV}, \\ m_N &= (920 \pm 100) \text{ MeV}. \end{aligned} \tag{38}$$

This fits the experimental low-lying hadron masses quite well. From the slope of (35) we also extract

$$f_\pi \approx 134 \text{ MeV} \tag{39}$$

using $m_\pi^2 f_\pi^2 = 4m_q \langle \bar{\psi}\psi \rangle_{\text{inv}}$ and our calculated value of $\langle \bar{\psi}\psi \rangle_{\text{inv}}$. This is to be compared to the experimental value of ⁽¹⁶⁾ $f_\pi = (131.9 \pm 0.1)\text{MeV}$

We have repeated our calculation at $\beta=5.4$ and 5.9 to check for continuum scaling behaviour⁽⁴⁰⁾. We find that the hadron masses scale within the statistical errors, except for the slope of the pion (35) at $\beta = 5.4$ which however has a natural explanation. We are also calculating the masses of various other states.

5. Concluding Remarks

We may say that altogether we begin to obtain a consistent picture of quark and gluon physics in quenched QCD, which is encouraging and more than we could expect on these rather coarse lattices and from working at the "edge" of the continuum region.

In the near future we will be able to double the sizes of our lattices, and we will have accumulated higher statistics. This will enable us to reduce the systematic uncertainties and the statistical errors. We are also beginning to make progress in including fermion loops.

Acknowledgements

I like to thank my colleagues Ian Barbour, Philip Gibbs, Philip Gilchrist, Kenzo Ishikawa, Heinz Schneider and Mike Teper for a most prolific collaboration and for continuous discussions on the subject of this talk.

References

1. K. Wilson: Phys. Rev. D10, 2445 (1974)
2. R.P. Feynman: Rev. Mod. Phys. 20, 267 (1948);
R.P. Feynman and A.R. Hibbs: Quantum Mechanics and Path Integrals (McGraw-Hill, 1965)
3. G. 't Hooft and M. Veltman: Diagrammar, CERN report 73-9 (1973)
4. K. Wilson and J. Kogut: Phys. Rep. 12C, 75 (1974)
5. M. Creutz: Phys. Rev. Lett. 43, 553 (1979);
K. Wilson: Cargese lectures (1979);
M. Creutz, L. Jacobs and C. Rebbi: Phys. Rev. D20, 1915 (1979)
6. For a recent review see:
M. Teper: talk at the Brighton conference (1983), and LAPP preprint TH-91 (1983)
7. M. Falcioni, E. Marinari, M.L. Paciello, G. Parisi, F. Rapuano, B. Taglienti and Zhang Yi-cheng: Phys. Lett. 110B, 295 (1982);
K. Ishikawa, G. Schierholz and M. Teper: Phys. Lett. 110B, 399 (1982);
B. Berg, A. Billoire and C. Rebbi: Ann. Phys. 142, 185 (1982)
8. K. Ishikawa, G. Schierholz and M. Teper: Zeitschr. f. Phys. C19, 69 (1982)
9. A. Hasenfratz and P. Hasenfratz: Phys. Lett. 93B, 165 (1980)
10. D.L. Scharre et al.: Phys. Lett. 97B, 329 (1980);
C. Edwards et al.: Phys. Rev. Lett. 48, 458 (1982);
ibid. 49, 259 (1982)
11. J.P. Gilchrist, G. Schierholz, H. Schneider and M. Teper: DESY preprint 83-094 (1983), to be published in Phys. Lett. B
12. For recent calculations on large lattices see:
M. Fukugita, T. Kaneko and A. Ukawa: KEK preprint TH 63 (1983);
F. Gutbrod, P. Hasenfratz, I. Montvay and Z. Kunszt: CERN preprint TH-3591 (1983)
13. G. Schierholz and M. Teper: in preparation;
see also ref.6
14. I.M. Barbour, P. Gibbs, J.P. Gilchrist, G. Schierholz, H. Schneider and M. Teper: DESY preprint 83-093 (1983), to be published in Phys. Lett. B
15. G. Launer, S. Narison and R. Tarrach: CERN preprint TH-3712 (1983)
16. J. Gasser and H. Leutwyler: Phys. Rep. 87C, 78 (1982)
17. J. Engels, F. Karsch, H. Satz and I. Montvay: Nucl. Phys. B205, 545 (1982);
J. Kogut, M. Stone, H.W. Wyld, W.R. Gibbs, J. Shigemitsu, S.H. Shenker and D.K. Sinclair: Illinois preprint TH-82-39 (1982)

18. K. Ishikawa, A. Sato, G. Schierholz and M. Teper: DESY preprint 83-061 (1983), to be published in Zeitschr. f. Phys. C
19. G. Schierholz and M. Teper: DESY preprint 83-107 (1983), to be published in Phys. Lett. B
20. K. Ishikawa, G. Schierholz and M. Teper: Phys. Lett. 116B, 429 (1982);
K. Ishikawa, A. Sato, G. Schierholz and M. Teper: Phys. Lett. 120B, 387 (1983)
21. B. Berg and A. Billoire: Phys. Lett. 113B, 65 (1982);
ibid. 114B, 324 (1982); Nucl. Phys. B221, 109 (1983)
22. B. Berg and A. Billoire: Nucl. Phys. B226, 405 (1983)
23. C. Michael and I. Teasdale: Nucl. Phys. B215, 433 (1983)
24. B. Lautrup and M. Nauenberg: Phys. Rev. Lett 45, 1755 (1980)
25. E. Bloom: talk at the Paris conference (1982)
26. See e.g. the reprint collection:
C. Rebbi: Lattice Gauge Theories and Monte Carlo Simulations (World Scientific, 1983)
27. K. Wilson: Erice lectures (1975)
28. L.H. Karsten and J. Smit: Nucl. Phys. B183, 103 (1981);
H.B. Nielsen and M. Ninomiya: Nucl. Phys. B185, 20 (1981)
29. J. Kogut and L. Susskind: Phys. Rev. D11, 395 (1975);
L. Susskind: Phys. Rev. D16, 3031 (1977);
T. Banks, J. Kogut and L. Susskind: Phys. Rev. D13, 1043 (1976);
T. Banks, S. Raby, L. Susskind, J. Kogut, D.R.T. Jones,
P.N. Scharbach and D. Sinclair: Phys. Rev. D15, 1111 (1976);
H.S. Sharatchandra, H.J. Thun and P. Weisz: Nucl. Phys. B192, 205 (1981)
30. N. Kawamoto and J. Smit: Nucl. Phys. B192, 100 (1981)
31. A. Duncan and R. Roskies: Pittsburgh preprint PITT-82-6 (1982);
P. Becher and H. Joos: Zeitschr. f. Phys. C15, 343 (1982);
T. Banks, Y. Dothan and D. Horn: Phys. Lett. 117B, 413 (1982);
H. Kluberg-Stern, A. Morel, O. Napoly and B. Petersson:
Saclay preprint DPh/83/29 (1983);
J. Kogut, M. Stone, H. Wyld, S. Shenker, J. Shigemitsu and
D. Sinclair: Illinois preprint DOE/ER/01545-335 (1983)
32. H. Kluberg-Stern, A. Morel, O. Napoly and B. Petersson: ref.31
33. I.M. Barbour, J.P. Gilchrist, G. Schierholz, H. Schneider and M. Teper: Phys. Lett. 127B, 433 (1983), and references therein
34. T. Jolicoeur, H. Kluberg-Stern, M. Lev, A. Morel and B. Petersson: Saclay preprint SPHT/83-70 (1983)

35. H. Hamber and G. Parisi: Phys. Rev. Lett. 47, 1792 (1981);
E. Marinari, G. Parisi and C. Rebbi: Phys. Rev. Lett. 47, 1795 (1981);
D. Weingarten: Phys. Lett. 109B, 57 (1982);
A. Hasenfratz, P. Hasenfratz, Z. Kunszt and C.B. Lang: Phys. Lett. 110B, 289 (1982)
36. D. Weingarten: Nucl. Phys. B215, 1 (1983);
F. Fucito, G. Martinelli, C. Omero, G. Parisi, R. Petronzio and F. Rapuano: Nucl. Phys. B210, 407 (1982);
R. Gupta and A. Patel: Caltech preprint 68-966 (1982);
A. Hasenfratz, P. Hasenfratz, Z. Kunszt and C.B. Lang: Phys. Lett. 117B, 81 (1982)
37. P. Hasenfratz and I. Montvay: Phys. Rev. Lett. 50, 309 (1983);
G. Martinelli, G. Parisi, R. Petronzio and F. Rapuano: Phys. Lett. 122B, 283 (1983);
R. Gupta and A. Patel: Phys. Lett. 124B, 94 (1983);
C. Bernard, T. Draper and K. Olynyk: Phys. Rev. D27, 227 (1983)
38. H. Lipps, G. Martinelli, R. Petronzio and F. Rapuano: CERN preprint TH-3548 (1983)
39. P. Hasenfratz and I. Montvay: DESY preprint 83-072 (1983)
40. J.P. Gilchrist, G. Schierholz, H. Schneider and M. Teper: in preparation